

## Article

# Adhesion of Varnish Coatings as a Background for Analogue and Digital Printing Technologies

Maciej Tokarczyk <sup>1,2</sup>, Barbara Lis <sup>1</sup>, Emilia Adela Salca <sup>3,\*</sup>  and Tomasz Krystofiak <sup>1,\*</sup>

<sup>1</sup> Department of Wood Science and Thermal Techniques, Faculty of Forestry and Wood Technology, Poznan University of Life Sciences, Wojska Polskiego 28, 60-627 Poznan, Poland; maciej.tokarczyk@up.poznan.pl (M.T.); barbara.lis@up.poznan.pl (B.L.)

<sup>2</sup> BORNE-FURNITURE Company, Złotego Smoka St. 23, 66-400 Gorzów Wielkopolski, Poland

<sup>3</sup> Faculty of Furniture Design and Wood Engineering, Transilvania University of Brasov, Universitatii 1, 500068 Brasov, Romania

\* Correspondence: emilia.salca@unitbv.ro (E.A.S.); tomasz.krystofiak@up.poznan.pl (T.K.)

**Abstract:** In analogue and digital printing technologies, from 3 up to 12 layers of lacquer products are applied. Technological parameters significantly influence the adhesion in the coating system. This article refers to the analysis of the influence of selected technological parameters, such as the number of layers, energy doses distributed by the radiators, and line speed, on the topography and adhesion of varnish coatings formed in the process of varnishing with rollers and UV-curing systems. The appropriately prepared surface can be used as a background layer for the analogue and digital printing technology. Manufacturers must adapt the production process to the particular varnish to obtain finished products with the best possible performance properties. The state of surface free energy and finally adhesion can be assessed by theoretically determining the possibility of an adhesive bonding between the product and the substrate, taking into account the assumptions of the adsorption theory of adhesion and measurement of the contact angle (Θ). An experimental confirmation of adhesion measurements included removing the coatings from the substrate via stamps glued to the coating.

**Keywords:** adhesion; analogue technology; printing technology; roughness; surface; topography; UV lacquer system; wettability



**Citation:** Tokarczyk, M.; Lis, B.; Salca, E.A.; Krystofiak, T. Adhesion of Varnish Coatings as a Background for Analogue and Digital Printing Technologies. *Appl. Sci.* **2024**, *14*, 304. <https://doi.org/10.3390/app14010304>

Academic Editor: Giuseppe Lazzara

Received: 30 November 2023

Revised: 24 December 2023

Accepted: 26 December 2023

Published: 29 December 2023



**Copyright:** © 2023 by the authors. Licensee MDPI, Basel, Switzerland. This article is an open access article distributed under the terms and conditions of the Creative Commons Attribution (CC BY) license (<https://creativecommons.org/licenses/by/4.0/>).

## 1. Introduction

The increasing shortage of wood promotes the development of technologies that apply other materials. Wood-based boards provide an excellent alternative to wood in the furniture industry, the advantage of which is a lower price and wide physical-mechanical parameters [1,2]. The properties of boards shaped during the technological process determine their application in various wood-processing industries. In the furniture and furnishing industry, MDF and HDF boards are widely used [3]. One of the many possibilities of using them in the production of furniture or interior doors made on cellular wood boards are the outer layers. The boards in their raw state are considered unattractive for various projects, so they are subjected to finishing via various methods. Analogue and digital printing techniques offer interesting solutions for increasing product attractiveness. In the former, the pattern carriers are engraved rollers, while in the latter, data in the digital form are transferred to the printhead [4–6]. UV varnish products, which are considered environmentally friendly, have been widely used in these technologies [5–10]. Their crosslinking occurs via polymerization based on a mechanism of free-radical reaction, which is initiated by UV radiation. Manufacturers need to adapt the production process to the particular varnish to obtain finished products with the best possible performance properties. Adhesion is one of the most important parameters determining the functional

properties and durability of a finish [11–13]. It is the result of the wetting and curing processes of varnish products on the substrate. Its value is influenced by a number of factors that can include the type and preparation of the substrate, the type of varnish, application, and curing parameters [14,15]. Adhesion can be assessed by theoretically determining the possibility of an adhesive bonding between the product and the substrate, taking into account the assumptions of the adsorption theory of adhesion and experimental studies. In theoretical terms, adhesion requires the determination of the work of adhesion ( $W_a$ ) and the surface free energy of the solid ( $\gamma_s$ ), taking into account their dispersive and polar components. To determine them, measurement of the contact angle ( $\Theta$ ) is used.

The contact angle depends on a number of factors, which include the type of film-forming polymer and its degree of cross-linking, the content of auxiliary agents, the type of substrate, and the surface roughness [16]. On the other hand, experimental measurements include removing the coatings from the substrate via stamps glued to the coating. For this purpose, manual, hydraulic, or pneumatic instruments are used. The results are given in numerical form (MPa), which expresses the minimum tensile stress required for detachment [14]. In the case of inadequate adhesion and cohesive strength, the coating will exhibit defects in the form of protruding from the substrate, contributing to the formation of incomplete products. Therefore, process parameters must be developed to ensure maximum adhesion, both between the substrate and the varnish coating and between the coatings of a given finish. The most important parameters include adjusting the thickness of the applied product, conveyor speed, radiator type, minimum radiation dose, and distance between the lamp and the substrate.

In addition, using very high line speeds poses quite a challenge in determining the above data to obtain the optimum degree of curing and coating properties. Many studies can be found in the references on this important technological issue of adhesion. They have focused, among other things, on the influence of surface preparation method, surface roughness [13,14,17–20], application technology, type of varnish product [11,13], the composition of varnish products [13,20–25], layer thickness [11,13], number of varnish coatings, and aging [20,26–32]. The wide range of experiments conducted previously proves the importance of this topic. The experiments illustrate what factors need to be considered when specifying process parameters for a quality product.

No results of studies devoted to this subject have been encountered in the literature for HDF surfaces finished with UV LED varnishes. It seems fully justified as work constantly is carried out on developing, improving, and implementing various UV varnish products in industrial practice and technology, and the scope of the undertaken projects is subject to the highest confidentiality clause. This constitutes a competitive advantage for the company. In this context, there is a legitimate need to research and develop an understanding of the phenomena of wetting and final adhesion.

This article is devoted to the analysis of the influence of selected technological parameters, such as the number of layers, energy doses distributed by the radiators, and line speed, on the adhesion of varnish coatings formed in the process of varnishing with a roller. The objective of this paper was implemented by evaluating the phenomenon of wetting on coatings formed on HDF board, determined based on the measurements of angle  $\Theta$ , the  $\gamma_s$ , and  $W_a$ , together with their dispersion and polar share, and experimentally using the pull-off method, taking into account the impact of the surface roughness on this process.

## 2. Materials and Methods

The surface finishing of a board with 100 × 60 cm HDF outer cladding was carried out with the roller method under the technological conditions of Borne Furniture. The application process of multilayer systems of varnish products was carried out at line feed rates of 25 and 40 m/min according to the general idea presented in Figure 1.

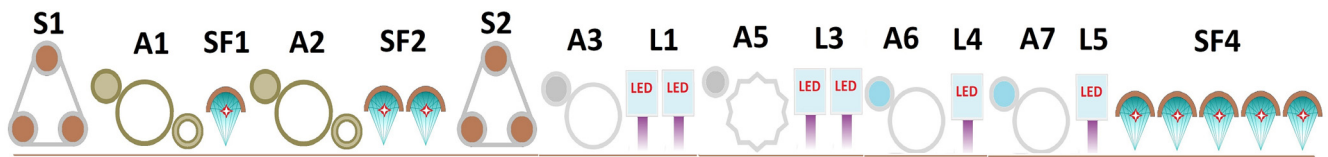


**Figure 1.** Selected schematic diagram for finishing the board furniture components with a roller method. Process description: (A1) putty 1–30 g/m<sup>2</sup>; (A2) putty 2–20 g/m<sup>2</sup>; (A3) basecoat 1–10 g/m<sup>2</sup>; (A5) basecoat 2–25 g/m<sup>2</sup>; (A6) topcoat 1–12 g/m<sup>2</sup>; (A7) topcoat 2–6 g/m<sup>2</sup>; (S1, S2) sanding; (L1, L3, L4, L5) LED lamp 396 nm 12 W/cm<sup>2</sup>; (SF1, SF2, SF4) super focus mercury lamp 120 W/cm.

Table 1 shows the basic properties of UV varnish products based on the manufacturer's technical sheets.

**Table 1.** Properties of UV varnish products.

Properties	Name of UV Varnish Products		
	Q-UV 03040 Putty	IQ-UVC03284 Basecoat	IQ-UVC03392 Topcoat
Polymer base	acrylic	acrylic	acrylic
Color	colorless	white	white
Solid content [%]	95.3 ± 3	97.6 ± 3	97.6 ± 3
Viscosity of delivery	65–85 (flow cup 8 mm)	90–140 (flow cup 6 mm)	35–50 (flow cup 6 mm)
Brookfield CAP 2000+/cone 2 [mPa·s]	1100–1500	-	-
Processing temperature [°C]	Between 20–50		

The templates prepared at different stages were transported to the laboratory, cut into samples, and left in an air-conditioned laboratory at 23 ± 2 °C, RH 50 ± 5% (Borne Furniture Company in Gorzow Wlkp. Poland). A summary of the samples with the accepted labeling is given in Table 2.

**Table 2.** Preparation of the test substrate.

Labeling of Samples (Systems)	Operations Performed in Preparation of the Test Substrate	Speed of Line [m/min]
1-3d	The surface of a cellular board with 1 layer 30 g/m <sup>2</sup> of a putty at the maximum setting of lamps focusing a beam of electromagnetic radiation	40
1-3a	The surface of a cellular board with 1 layer 30 g/m <sup>2</sup> of a putty at the maximum setting of lamps focusing a beam of electromagnetic radiation	25
1-7d	The surface of a cellular board with 1 layer of a filler with increased input, 1 layer of a filler with decreased input, and 1 primer at the maximum setting of lamps focusing a beam of electromagnetic radiation behind the 2 filler and maximum setting of LED modules behind the 1 basecoat 20 g/m <sup>2</sup>	40
1-7a	The surface of a cellular board with 1 layer of a filler with increased input, 1 layer of a filler with decreased input, and 1 primer at the maximum setting of lamps focusing a beam of electromagnetic radiation behind the 2 filler and maximum setting of LED modules behind the 1 basecoating 20 g/m <sup>2</sup>	25
1-8d	The surface of a cellular board with 1 layer of a putty with increased input, 1 layer of a filler with decreased input, and 1 primer at 50% setting of lamps focusing a beam of electromagnetic radiation behind the 2 filler and maximum setting of LED modules behind the 1 basecoating 10 g/m <sup>2</sup>	40

Table 2. Cont.

Labeling of Samples (Systems)	Operations Performed in Preparation of the Test Substrate	Speed of Line [m/min]
1-8a	The surface of a cellular board with 1 layer of a putty with increased input, 1 layer of a putty with decreased input, and 1 primer at 50% setting of lamps focusing a beam of electromagnetic radiation behind the 2 filler and maximum setting of LED modules behind the 1 basecoating 10 g/m <sup>2</sup>	25
1-14d	The surface of a cellular board with 2 layers of a putty, 2 layers of a primer using OPTI, and 2 layers of topcoat 12 g/m <sup>2</sup> at the maximum setting of lamps focusing a beam of electromagnetic radiation and maximum for each LED module.	40
1-14a	The surface of a cellular board with 2 layers of a putty, 2 layers of a primer using OPTI, and 2 layers 12 g/m <sup>2</sup> of topcoat at the maximum setting of lamps focusing a beam of electromagnetic radiation and maximum for each LED module.	25
1-15d	The surface of a cellular board with 2 layers of a putty, 2 layers of a primer using OPTI, and 1 layer 6 g/m <sup>2</sup> of topcoat at the maximum setting of lamps focusing a beam of electromagnetic radiation and maximum for each LED module.	40
1-15a	The surface of a cellular board with 2 layers of a putty, 2 layers of a primer using OPTI and 1 layer of topcoat 6 g/m <sup>2</sup> at the maximum setting of lamps focusing a beam of electromagnetic radiation and maximum for each LED module.	25

After that, the visual assessment was carried out and the following measurements were taken: topographic, surface roughness, contact angle, and adhesion.

### 2.1. Visual Assessment

Visual assessment was conducted with an unaided eye at a distance of 250 mm, incident at an acute angle to highlight the presence of potential surface defects.

### 2.2. Surface Topography

Surface topography was measured with a OneAttention Theta optical tensiometer (Biolin Scientific AB, Västra Frölunda, Sweden). The parameters of the measurement system are given in Table 3.

Table 3. Measurement system's parameters [33].

Method	Fringe Projection Phase-Shifting
XY pixel size	1.1 µm × 1.1 µm
Measured range in Z direction	1–60 µm
Lateral sampling (XY)	1.41 mm × 1.06 mm
Measurement speed	5–30 s (1280 × 960 measurement points)
Imaging options	Optical image, 2D and 3D roughness graphs
Method	Fringe projection phase-shifting
XY pixel size	1.1 µm × 1.1 µm
Measured range in Z direction	1–60 µm
Lateral sampling (XY)	1.41 mm × 1.06 mm

### 2.3. Roughness

A SJ-210 profilometer was applied to test the geometric structure of the surface. Specialized software (Version; SJ-210 V.1.000) was also used, and it aimed to control the profilometer and determine the numerical values of roughness parameters. The element that represented the surface was a diamond blade with an apex angle of 60° and a radius of 2 µm. Prior to the experiment, the profilometer was calibrated according to the roughness standard ISO 4287-1998 [34]. After that, the measurement conditions were entered, and the roughness parameters were specified (speed 0.5 mm/s, ln = 12.5 mm (length of the measur-

ing section), and  $\lambda_c = 0.25$  mm (cut-off)). Three indices were determined:  $R_a$ —asymmetric mean of the profile ordinates,  $R_z$ —roughness height according to 10 points,  $R_{max}$ —highest profile height.

#### 2.4. Contact Angle

Measurements were carried out with a PG3 goniometer using distilled water (at a temperature of 20 °C) as the wetting liquid according to the PN-EN 828 standard [35]. A water droplet with a volume of 3.5  $\mu\text{L}$  was applied to the surface with an integrated micro dosing pump and the camera recorded its behavior in contact with the substrate for 60 s. Based on the data obtained, specialized software analyzed the droplet's shape by determining the contact angle's value. Building upon the data of the contact angle obtained for a water droplet stabilized for 10 s and in compliance with the assumptions of the adsorption theory of adhesion, the interactions between the substrate–individual layers of coating system of the values of surface free energy ( $\gamma_s$ ) and work of adhesion ( $W_a$ ), together with the dispersive and polar components, were determined [16].

#### 2.5. Adhesion of Coatings

The test was carried out in compliance with EN ISO 4624 [36]. Silane epoxy adhesive (viscosity 50,000 mPa·s, processing time 30 min, handling strength after 120 min) from Jowat Polska Company was used to glue stamps measuring 20 mm in diameter to the test surfaces. After a conditioning period of 168 h, the surfaces of the specimens were notched around the measuring stamps using a hob cutter. They were then peeled off with a hydraulically driven PostiTest test apparatus. Nine tests were carried out on each test system. The images of delamination under destructive loads were assessed visually, taking into account the rating scale in Table 4.

**Table 4.** Measurement system's parameters [36].

Detachment Type	Detachment Occurring in a Given System
A	Cohesive in a substrate
A/B	Adhesive between a substrate and the first coating
B	Cohesive in the first coating
B/C	Adhesive between the first and second coating
-/Y	Adhesive of the last coating and glue
Y	Cohesive in glue
Y/Z	Adhesive between glue and a measuring stamp

### 3. Results

The resulting systems were of high quality, with no defects registered, which indicates that the substrate finishing stages were carried out correctly. In addition, no defects were observed after their transport to the testing laboratory, which confirms the adequate delivery conditions and control over the mode of transport. When assessing the appearance of the surface, an increase in the homogeneity of the varnish coating was observed in the function of the applied coatings.

#### 3.1. Visual Assessment

The visual assessment of the tested systems was complemented by quality verification based on tactile sensations. In contact with the hand, the final coatings evoked a pleasant tactile sensation and sensory satisfaction. It is notable that this effect is of great importance to furniture users. As an example, Table 5 shows a graphical representation of the surfaces of the tested systems.

Table 5. Image of surface topography with a travel rate of 25 m/min.

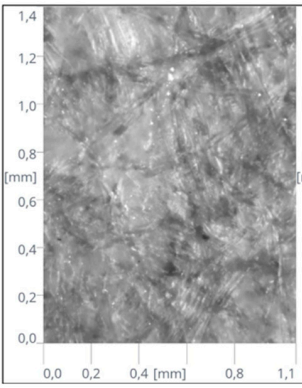
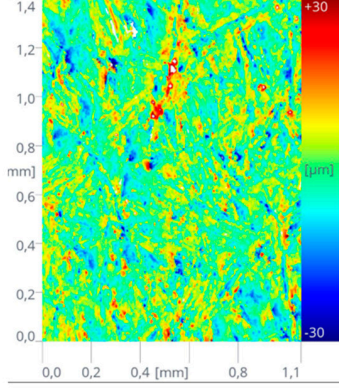
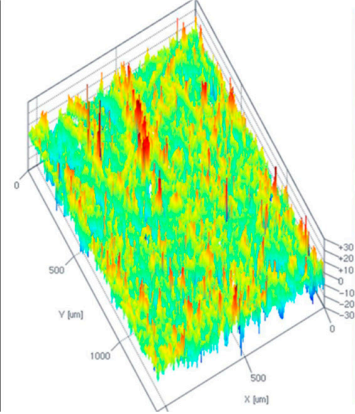
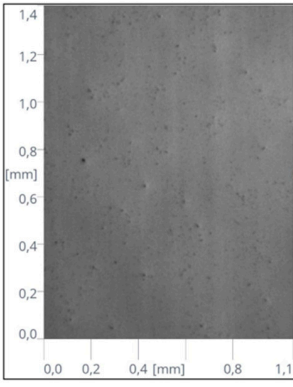
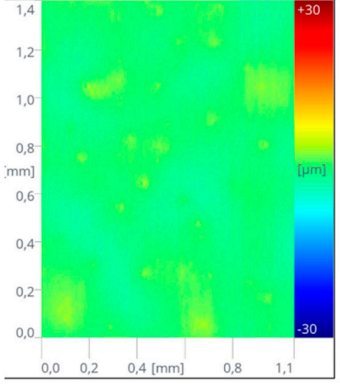
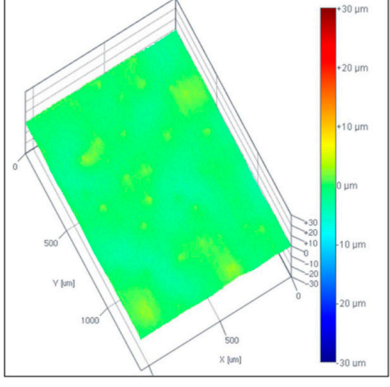
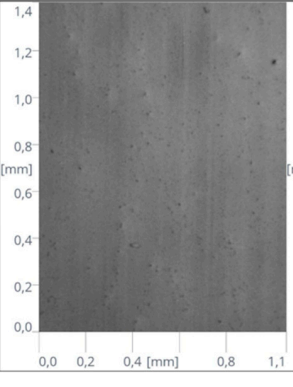
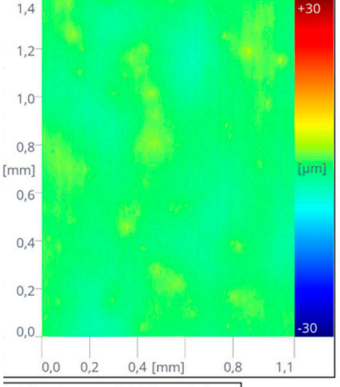
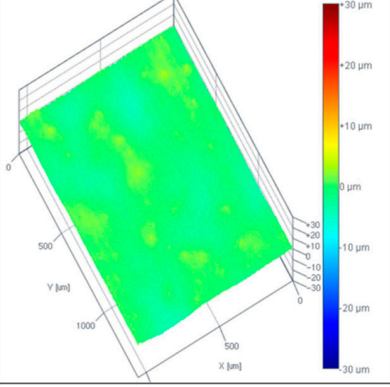
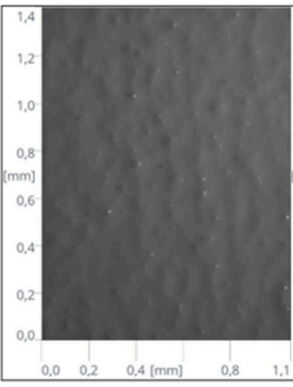
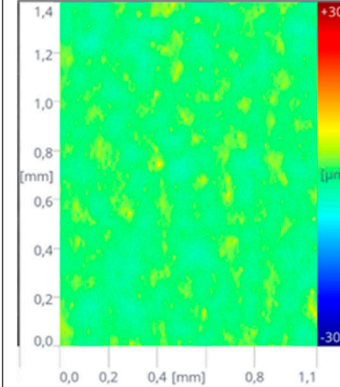
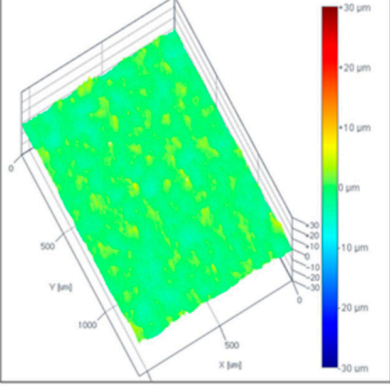
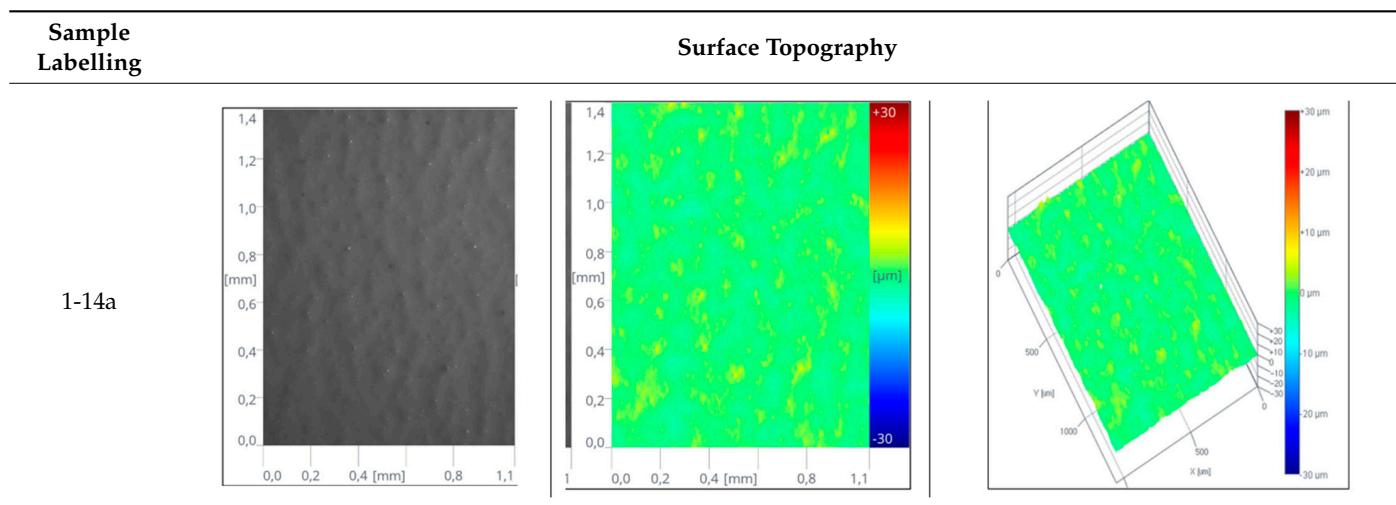
Sample Labelling	Surface Topography		
1-3a			
1-7a			
1-8a			
1-14a			

Table 5. Cont.



On the topographic images of the selected surfaces, it can be seen that both the applied layers and the applied doses of energy distributed by the radiators influenced the surface structure. The recorded changes were visible in the roughness measurements. However, the study showed values of final coatings that were unexpectedly higher than the values of primers. The average values of 10 measurements of the recorded roughness parameters are shown in Figure 2.

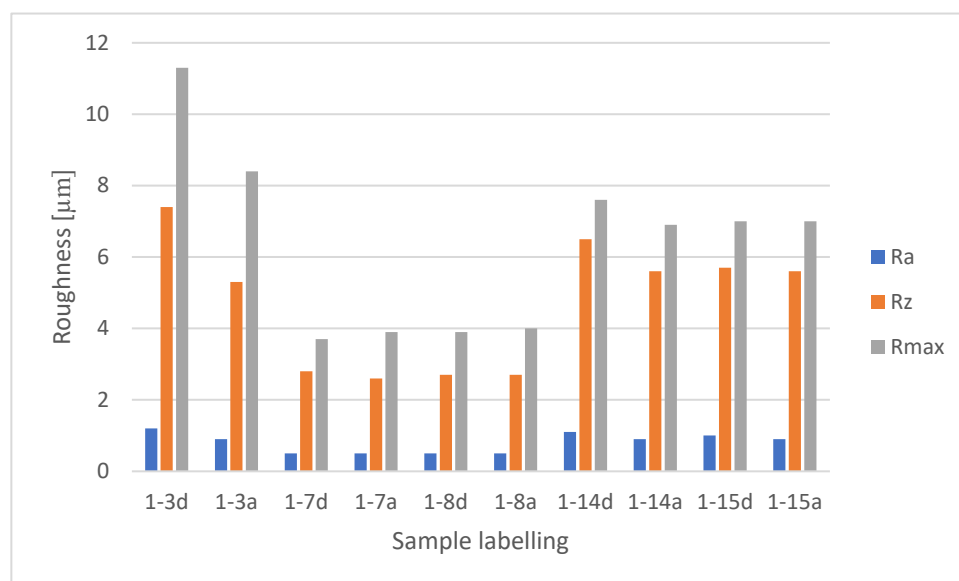


Figure 2. Values of Ra, Rz, and Rmax parameters for the tested systems.

From the results obtained, it can be observed that the determined average values of the Ra parameter, irrespective of the tested system, were approximately six times lower than Rz. In addition, lower values were found for the interlayer systems with the exception of the one layer of putty (systems 1-3). It is most likely that this layer, which is in direct contact with the HDF board despite the doubled input, penetrated the substrate, which influenced the recorded parameters. Studies conducted by Bialecki et al. in 2008 [37] proved the influence of the structure of the HDF board on the amount of varnish applied to achieve an adequate surface preparation. Parameters that were indicative of the above correlation were the selected roughness indices. This would confirm the penetration of the putty deep into the board while creating a rougher surface. The application of an increased

putty layer, a second putty layer, sanding, and a primer layer reduced the roughness level by almost half regardless of the conveyor speed. For the final coatings, the roughness was almost an order of magnitude higher than the systems with putty and primer layers. However, with regard to the one putty layer, they showed similar values to the determined indices. This could be due to the different rheological properties of the applied products, different energy doses distributed by the radiators, the reduction in product volume, and their shrinking during the polymerization process [38–40]. The geometrical structure of the surface, shaped in the technological process, can influence the wetting processes. This relationship is indicated in the references [41,42].

### 3.2. Contact Angle

Figure 3 presents the average contact angle values as a function of the Ra parameter.

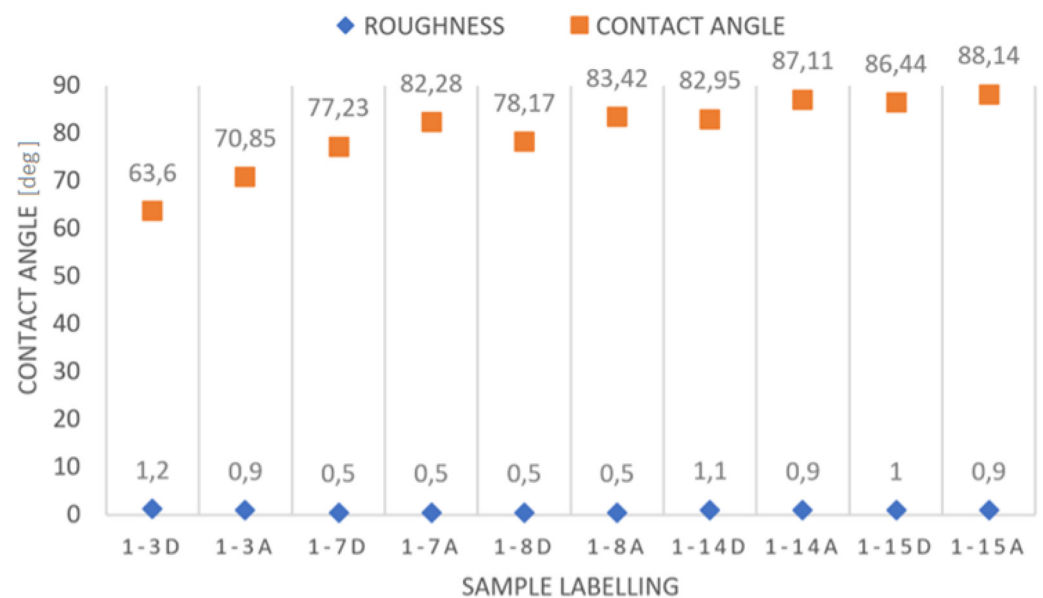


Figure 3. Formation of contact angle for the tested systems.

However, no unambiguous correlations between the change in contact angle and the recorded roughness index were found in the studies. The mechanisms of interaction between selected technological parameters do not enable us to determine the reasons for such discrepancies unambiguously. The coating formed from one putty layer at the assumed process parameters is characterized by the highest roughness. In this case, the hydrophobic character of the surface was weakened, which ensured good adhesion properties for the subsequent layers. Further layer application resulted in a decrease in wettability, which contributed to increased contact angle. Although final coatings exhibited a similar roughness to the system with one layer of putty, the contact angle was not reduced. In addition, it was observed that the systems prepared at varying conveyor speeds showed slight differences in the formation of the recorded values. These differences are due to the doses of energy distributed as a result of the longer residence of the samples under the radiator. Different levels for different speeds were also recorded between primer systems. The smallest impact of speed was observed in the case of topcoat systems. This is undoubtedly related to the type of products and their composition. In general, systems with undercoats only had lower values than final coatings with topcoats. From the point of view of the technological process, this is very advantageous. The contact area between the liquid and the substrate is then greater. Therefore, it can be indirectly concluded that the varnish products will have the ability to wet the substrate and achieve a favorable adhesive bond between the wetted material and the varnish coatings [43,44]. On the other hand, the recorded higher contact angle contributes to the formation of hydrophobic properties of the topcoats, which is desirable during the use of the final products. When considering the

evaluated parameter as a function of the number of coatings applied, the lowest values were found for one putty coating at the maximum lamp setting regardless of the conveyor speed. An increase in this parameter was recorded with the application of subsequent layers. This is due to an increase in the homogeneity of the varnish coating and the deliberate action of changing the energy density supplied during the refinement process. Coatings that are less cross-linked are more wettable and, at the same time, more susceptible to sanding. The sanding process is an advisable treatment after the application of putty layers. With regard to the systems considered, the highest angle value was achieved by system 1-15a consisting of five coatings comprising two layers of putty and primer using the OPTI and one layer of topcoating  $6 \text{ g/m}^2$  at the maximum settings of the electromagnetic beam focusing lamps and for each LED module (Table 6). The observed differences for each system are the result of different energy doses of absorbed electromagnetic radiation. In addition, it was noted that the use of higher conveyor speeds contributes to lower values of the contact angle, which is undoubtedly related to the absorption of different energy doses (Figure 4).

Table 6. UV curing system measurement.

Samples	Speed [m/min]	Amount for Last Layer [g/m <sup>2</sup> ]	Type	Wavelength Range	Power Peak [mW/cm <sup>2</sup> ]	Energy Density [mJ/cm <sup>2</sup> ]
1-3d	40	30	putty	UVV UVA	1050 1155	85 90
1-3a	25	30	putty	UVV UVA	1065 1170	135 150
1-7d	40	20	basecoat	UVV	11,550	575
1-7a	25	20	basecoat	UVV	11,567	922
1-8d	40	10	basecoat	UVV	11,550	575
1-8a	25	10	basecoat	UVV	11,567	922
1-14d	40	12	topcoat	UVV UVA	7050 2860	505 305
1-14a	25	12	topcoat	UVV UVA	7050 2860	800 490
1-15d	40	6	topcoat	UVV UVA	7050 2860	505 305
1-15a	25	6	topcoat	UVV UVA	7050 2860	810 485

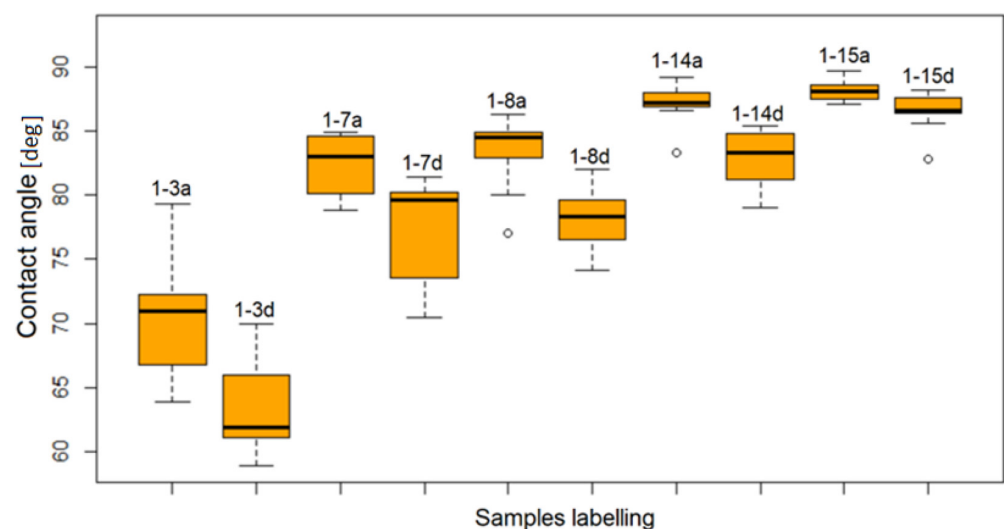


Figure 4. Contact angle's result.

A correlation analysis based on Tukey's criterion multiple comparisons of means with a 95% confidence level shows that the energy density applied to the surface has an influence on the formation of the contact angle. In many cases, for the same type of applied materials, no effects of changing the application amount on the contact angle were observed. The small impact of the amount of liquid materials applied on the surface with the same energy density was observed between the topcoat, samples 1-14d (12 g/m<sup>2</sup>), and 1-15d (6 g/m<sup>2</sup>).

The type of varnish used clearly influences the formation of the contact angle between the basecoating with a mean of 82.28° (1-7a) and the topcoating with a mean of 87.11° (1-14a), (*p*-value 0.0103271).

Additionally, it was stated that line speed has equal importance on the formation of the contact angle with the same power of lamp. For example, the mean of 63.60° for 1-3d at 40 m/min in comparison to 70.85° for 1-3a at 25 m/min (*p*-value 0.0000077) or the mean of 77.23° for 1-7d at 40 m/min in comparison to 82.28° for 1-7a at 25 m/min (*p*-value 0.0058). The samples stay under the lamps longer, which affects the density of energy supplied to the process.

Based on the value of the contact angle, a parameter characterizing the wetting process of the substrate ( $\gamma_S$ ) with the varnish products and the interlayer interaction was calculated. It indicates the possibility of systems with compatible relations between the individual layers.

Preliminary analysis of the values of surface free energy influencing the adsorption, wetting, and adhesion processes to the most significant extent, being at the same time the effect of intermolecular interactions, indicates that the tested systems exhibited  $\gamma_S$  values in the range of 32–51 mJ/m<sup>2</sup> (Figure 5). Regarding the theoretical assumptions of the adsorption theory of polymer adhesion to the substrate, the  $\gamma_S$  value of the refined surface should be higher than that of the consolidated varnish. In the evaluated relations, this requirement was fulfilled. Based on literature data, for the HDF board, the values for beech wood (*Fagus sylvatica* L.) of  $\gamma_S = 67.6$  mJ/m<sup>2</sup>,  $\gamma_S^d = 24.7$  mJ/m<sup>2</sup>, and  $\gamma_S^p = 42.9$  mJ/m<sup>2</sup> [16], on which the HDF board was based, were adopted. This allowed an indirect inference about the  $\gamma_S$  value of the HDF board despite the use of adhesive and hydrophobic agents in its production. The obtained  $\gamma_S$  values exceeded the relevant data determined for the varnish coatings under consideration.

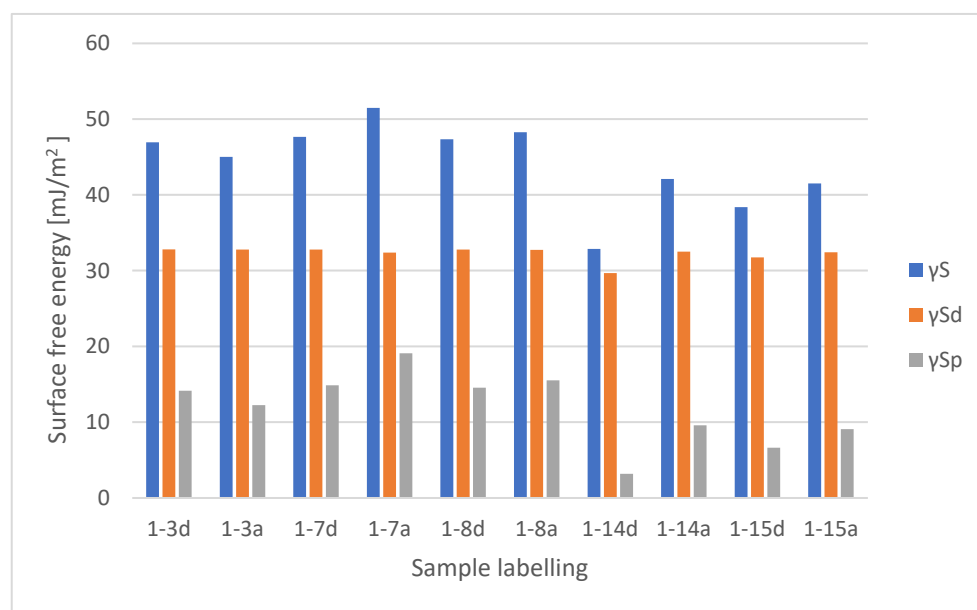


Figure 5. Results of the surface free energy.

When evaluating the relations between the applied products, interlayer coatings were characterized by higher  $\gamma_S$  values. The primer coatings can therefore be regarded as a

typically intermediate factor in shaping the final adhesion. The application of topcoats resulted in a decreased surface energy. A clear influence of the dispersion component on the formation of  $\gamma_S$  values was found. After the phase transformation of the products into solidified layers, the resulting varnish coatings were characterized by favorable interlayer adhesion and substrate adhesion.

Unevenness and porosity increase the effective interaction surface between the surface forces of the substrate and varnish products and, therefore, increase the value of the work of adhesion of the varnish to the board compared to the work of adhesion and spreading of the varnish on a smooth surface. The work of adhesion ( $W_a$ ) in the HDF-coat varnish system had a higher value (91.80–93.78 mJ/m<sup>2</sup>) than the work of adhesion of the topcoats to the primers (75.79 to 87.82 mJ/m<sup>2</sup>). The primer coatings can, therefore, be regarded as a factor typically facilitating the formation of the final adhesion. Considering the values of the dispersion component of the work of adhesion ( $W_{ad}$ ) for the systems under consideration, it was found that they were quite similar at 65 mJ/m<sup>2</sup>, while the polar component of the work of adhesion ( $W_a^p$ ) varied considerably. The results obtained for the variants under consideration, including both  $W_a$  and its components  $W_{ad}$  and  $W_a^p$ , provide, as regards theoretical possibilities, favorable conditions to obtain varnish coatings exhibiting high adhesion in both interlayer and final systems in the finishing process. This was confirmed in pull-off adhesion tests.

Moreover, this parameter was found to be higher than the surface roughness. Furthermore, it was shown that the substrate, i.e., the cohesive forces of the HDF board, was predominantly the weakest link in the tested systems. This can be explained by the fact that the contact area between the substrate and the solidified putty layer increases with increasing roughness. In addition to this, it should be taken into account that on a rough surface, the putty layer may have a higher affinity with the surface. The observed relationships are confirmed by the mechanical theory of adhesion developed by Mc Bain and Hopkins in 1925 [45,46], according to which decohesion occurs within the bonded materials, among others, as a result of anchoring the applied product into the rough surface and not at the interface. The finishes' quality can be considered fully acceptable in light of the results obtained.

#### 4. Conclusions

Research material has been previously presented on the patented technological line [47]. The obtained results in the current study are difficult to relate to the data of other authors since adhesion evaluation for varnish coatings of UV LED products formed on HDF boards under industrial conditions has not been carried out. In the surface interactions of the cured systems in the substrate–varnish products relationship, in terms of the adhesion phenomenon, the following was found:

1. Tested surfaces were characterized by  $R_a$  values in the range of 0.5–1.2  $\mu\text{m}$ , and contact angle  $\theta$  was in the range of  $63.60 \div 88.14^\circ$  for individual surfaces.
2. The power of the radiators and speed of the line have a greater influence on the formation of the contact angle than the amount of liquid materials applied on each roller machine.
3. The speed of the line is important for the formation of the contact angle at the same power of the lamp.
4. No correlation between the change in the contact angle and recorded roughness index was observed.
5. Final coatings exhibited lower  $\gamma_S$  values than interlayer coatings. A clear influence of the dispersion component on the formation of  $\gamma_S$  values was observed. No clear effect of the applied curing parameters on the value of the  $\gamma_S^d$  component was noted.
6. The obtained coatings were characterized by high  $W_a$  values, ranging from 75.79–97.94 mJ/m<sup>2</sup>. For the individual systems, the level of  $W_a$  values achieved depended primarily on the type of individual varnish product layers. The relationship

- between  $W_a$  and its components,  $W_{ad}$  and  $W_{aP}$ , provided favorable conditions for obtaining coatings with high adhesion in the finishing process.
7. The adhesion of individual layers to the HDF board's surface and the interlayer system in the analyzed systems ranged from 1.25–1.56 MPa. However, cohesive-type delamination in the HDF board was clearly the dominant delamination mechanism under destructive loads.
  8. The substrate refinement parameters adopted in the roller refinement provide favorable conditions for obtaining final finishes in terms of adequate adhesion. This applies to the doses of energy distributed by the radiators, in Ga, Hg, and LED versions, the module focusing the electromagnetic radiation beam, and the distance of the radiator from the cured surface layers and varnish coatings.

**Author Contributions:** Conceptualization, M.T. and T.K.; methodology, M.T., B.L. and T.K.; software, M.T.; validation, M.T., B.L. and T.K.; formal analysis, M.T.; investigation, M.T. and B.L.; resources, M.T., B.L. and T.K.; data curation, M.T.; writing—original draft preparation, M.T., B.L. and T.K.; writing—review and editing, M.T., B.L., E.A.S. and T.K.; visualization, M.T.; supervision, B.L. and T.K.; project administration, M.T., B.L. and T.K.; funding acquisition, M.T. All authors have read and agreed to the published version of the manuscript.

**Funding:** This research was funded by the Borne Furniture Company in Gorzow Wielkopolski Poland and the APC was funded by the same company.

**Institutional Review Board Statement:** Not applicable.

**Informed Consent Statement:** Not applicable.

**Data Availability Statement:** The data presented in this study is available upon request from the corresponding author. The data are not publicly available due to privacy.

**Acknowledgments:** The authors would like to gratefully acknowledge the National Center for Research and Development (Poland). All samples were prepared by using the finishing UV-curing line created as a result of research and development works of project POIR.01.01.01-00-1235/17, Development of technology for finishing the surface of wood materials using selected energy-saving sources electromagnetic radiation at advanced speeds and varnish systems characterized by increased resistance.

**Conflicts of Interest:** Author Maciej Tokarczyk was employed by the BORNE-FURNITURE Company. The remaining authors declare that the research was conducted in the absence of any commercial or financial relationships that could be considered as a potential conflict of interest. The authors declare that this study received funding from Borne Furniture Company. The funder was not involved in the study design, collection, analysis, interpretation of data, the writing of this article or the decision to submit it for publication.

## References

1. Bartoszek, K.; Kowaluk, G. The Influence of the Content of Recycled Natural Leather Residue Particles on the Properties of High-Density Fiberboards. *Materials* **2023**, *16*, 5340. [[CrossRef](#)] [[PubMed](#)]
2. Henke, M.; Lis, B.; Krystofiak, T. Mechanical and Chemical Resistance of UV Coating Systems Prepared under Industrial Conditions. *Materials* **2023**, *16*, 4468. [[CrossRef](#)] [[PubMed](#)]
3. Rahaman, M.; Hossain, S.; Islam, M.; Uddin, M. Suitability of Medium Density Fiber Board Made From Rubber Wood for Household and Industrial Use. *Bangladesh J. Agric. Res.* **2021**, *46*, 203–209. [[CrossRef](#)]
4. Pawlak, D.; Boruszewski, P. Digital printing in wood industry. *Ann. WULS For. Wood Technol.* **2020**, *109*, 109–115. [[CrossRef](#)]
5. Sang, R.; Manley, A.; Wu, Z.; Feng, X. Digital 3D Wood Texture: UV-Curable Inkjet Printing on Board Surface. *Coatings* **2020**, *10*, 1144. [[CrossRef](#)]
6. Mendes, C.; Oliveira, J.; Etxebarria, I.; Vilas, J.; Lanceros-Méndez, S. State-of-the-Art and Future Challenges of UV Curable Polymer-Based Smart Materials for Printing Technologies. *Adv. Mater. Technol.* **2019**, *4*, 1800618. [[CrossRef](#)]
7. Altun, S.; Köse, D. Some of the Physical Properties of UV Jet Printed Furniture Surfaces. *Drv. Ind.* **2013**, *64*, 39–43. [[CrossRef](#)]
8. Rawat, R.S.; Nidhi Chouhan, N.; Talwar, M.; Diwan, R.K.; Tyagi, A.K. UV coatings for wooden surfaces. In *Progress in Organic Coatings*; MDPI: Basel, Switzerland, 2019; Volume 135, pp. 490–495. ISSN 0300-9440. [[CrossRef](#)]

9. Lu, Q.; Zhang, C.; Huang, B.; Wei, X.; Wang, Y. Study on the Application of UV Ink in Printing Manufacturing. In *Advances in Graphic Communication, Printing and Packaging Technology and Materials*; Springer: Berlin/Heidelberg, Germany, 2021; pp. 629–636. [\[CrossRef\]](#)
10. Sang, R.; Yang, S.; Fan, Z. Effects of MDF Substrate Surface Coating Process on UV Inkjet Print Quality. *Coatings* **2023**, *13*, 970. [\[CrossRef\]](#)
11. Ozdemir, T.; Bozdoğan, Ö.; Mengelöglu, F. Effects of Varnish and Film Thickness on Adhesion Strength of Coated Wood. *Pro ligno* **2013**, *9*, 164–168.
12. Nkeuwa, W.N.; Riedl, B.; Landry, V. Wood surfaces protected with transparent multilayer UV-cured coatings reinforced with nanosilica and nanoclay. Part I: Morphological study and effect of relative humidity on adhesion strength. *J. Coat Technol. Res.* **2014**, *11*, 283–301. [\[CrossRef\]](#)
13. Kılıç, K.; Söğütü, C. Varnish Adhesion Strength in Natural Aged Wood Material. *Politek. Derg. J. Polytech.* **2023**, *26*, 847–854. [\[CrossRef\]](#)
14. Vitosytė, J.; Ukvalbergienė, K.; Keturakis, G. The Effects of Surface Roughness on Adhesion Strength of Coated Ash (*Fraxinus excelsior* L.) and Birch (*Betula* L.) Wood. *Mater. Sci.* **2012**, *18*, 347–351. [\[CrossRef\]](#)
15. Iis, Y.; Istie, R.; Lumongga, D.; Darmawan, W. Wettability and adherence of acrylic paints on long and short rotation teaks. *Wood Mater. Sci. Eng.* **2019**, *15*, 229–236. [\[CrossRef\]](#)
16. Pecina, H.; Paprzycki, O. Lack auf Holz. In *Lacquers on the Wood*; Vincentz Verlag: Hannover, Germany, 1995; p. 175.
17. Ozdemir, T.; Hiziroglu, S. Evaluation of surface quality and adhesion strength of treated solid wood. *J. Mater. Process. Technol.* **2007**, *186*, 311–314. [\[CrossRef\]](#)
18. Ozdemir, T.; Hiziroglu, S. Influence of surface roughness and species on bond strength between the wood and the finish. *For. Prod. J.* **2009**, *59*, 90–94.
19. Ozdemir, T.; Hiziroglu, S.; Kocapınar, M. Adhesion Strength of Cellulosic Varnish Coated Wood Species as Function of Their Surface Roughness. *Adv. Mater. Sci. Eng.* **2015**, *2015*, 525496. [\[CrossRef\]](#)
20. Guo, X.; Li, R.; Teng, Y.; Cao, P.; Wang, X.; Ji, F.; Vohringer, S. Effects of surface treatment on the properties of UV coating. *Wood Res.* **2015**, *60*, 629–638.
21. Jung, S.J.; Lee, S.J.; Cho, W.J.; Ha, C.S. Synthesis and properties of UV-curable waterborne unsaturated polyester for wood coating. *J. Appl. Polym. Sci.* **1998**, *69*, 695–708. [\[CrossRef\]](#)
22. Mashouf, G.; Ebrahimi, M.; Bastani, S. UV curable urethane acrylate coatings formulation: Experimental design approach. *Pigment Resin Technol.* **2014**, *43*, 61–68. [\[CrossRef\]](#)
23. Dai, J.; Ma, S.; Wu, Y.; Liu, X. High bio-based content waterborne UV-curable coatings with excellent adhesion and flexibility. *Prog. Org. Coat.* **2015**, *87*, 197–203. [\[CrossRef\]](#)
24. Dai, J.; Ma, S.; Liu, X.; Han, L.; Wu, Y.; Dai, X.; Zhu, J. Synthesis of bio-based unsaturated polyester resins and their application in waterborne UV-curable coatings. *Prog. Org. Coat.* **2015**, *78*, 49–54. [\[CrossRef\]](#)
25. Yan, X.; Qian, X.; Lu, R.; Miyakoshi, T. Synergistic Effect of Addition of Fillers on Properties of Interior Waterborne UV-Curing Wood Coatings. *Coatings* **2018**, *8*, 9. [\[CrossRef\]](#)
26. Gurleyen, L.; Ayata, U.; Esteves, B.; Cakicier, N. Effects of heat treatment on the adhesion strength, pendulum hardness, surface roughness, color and glossiness of Scots pine laminated parquet with two different types of UV varnish application. *Maderas. Cienc. Y Tecnol.* **2017**, *19*, 213–224. [\[CrossRef\]](#)
27. Çavuş, V. Weathering Performance of Mulberry Wood with UV Varnish Applied and Its Mechanical Properties. *Bioresources* **2021**, *16*, 6791–6798. [\[CrossRef\]](#)
28. Bekhta, P.; Lis, B.; Krystofiak, T.; Tokarczyk, M.; Bekhta, N. Gloss of Varnished MDF Panels Veneered with Sanded and Thermally Compressed Veneer. *Coatings* **2022**, *12*, 913. [\[CrossRef\]](#)
29. Salca, E.A.; Krystofiak, T.; Lis, B.; Mazela, B.; Proszek, S. Some Coating Properties of Black Alder Wood as a Function of Varnish Type and Application Method. *Bioresources* **2016**, *11*, 7580–7594. [\[CrossRef\]](#)
30. Hazir, E.; Koc, K.H. Evaluation of wood-based coating performance for ultraviolet roller and conventional air-atomization processes, *Maderas. Cienc. Y Tecnol.* **2021**, *23*, 1–16. [\[CrossRef\]](#)
31. Kaygin, B.; Akgun, E. Comparison of Conventional Varnishes with Nanolack UV Varnish With Respect to Hardness and Adhesion Durability. *Int. J. Mol. Sci.* **2008**, *9*, 476–485. [\[CrossRef\]](#)
32. Gürleyen, L. Effects of Artificial Weathering on the Color, Gloss, Adhesion, and Pendulum Hardness of UV System Parquet Varnish Applied to Doussie (*Azalia africana*) Wood. *Bioresources* **2021**, *16*, 1616–1627. [\[CrossRef\]](#)
33. *Anonymous Theta Flex User Manual—OneAttention Original Instructions*; Biolin Scientific Oy: Espoo, Finland, 2019; p. 74.
34. *ISO 4287 (1998)*; Geometrical Product Specification (GPS)—Surface Texture: Profile Method—Terms, Definitions and Surface Texture Parameters. International Organization for Standardization: Geneva, Switzerland, 1998.
35. *PN-EN 828*; Adhesives—Determination of Wettability by Measuring the Contact Angle and Surface Free Energy of a Solid Surface. iTeh Standard: Etobicoke, ON, Canada, 2013.
36. *PN-EN 4624*; Paints and Varnishes—Pull-Off Test for Adhesion. iTeh Standard: Etobicoke, ON, Canada, 2023.
37. Bialecki, F.; Pohl, P.; Sydor, M. Investigations on sealing material consumption in relation with the roughness parameters of HDF boards. *EJPAU* **2008**, *11*, 17.

38. Park, J.W.; Shim, G.S.; Lee, J.G.; Jang, S.W.; Kim, H.J.; Choi, J.N. Evaluation of UV Curing Properties of Mixture Systems with Differently Sized Monomers. *Materials* **2018**, *11*, 509. [[CrossRef](#)] [[PubMed](#)]
39. Park, J.W.; Shim, G.S.; Back, J.H.; Kim, H.J.; Shin, S.; Hwang, T.S. Characteristic shrinkage evaluation of photocurable materials. *Polym. Test.* **2016**, *56*, 344–353. [[CrossRef](#)]
40. Sanai, Y.; Ninomiya, T.; Arimitsu, K. Improvements in the physical properties of UV-curable coating by utilizing type II photoinitiator. *Prog. Org. Coat.* **2021**, *151*, 106038. [[CrossRef](#)]
41. Papp, E.; Csiha, C. Contact angle as function of surface roughness of different wood species. *Surf. Interfaces* **2017**, *8*, 54–59. [[CrossRef](#)]
42. Yu, Q.; Pan, X.; Yang, Z.; Zhang, L.; Cao, J. Effects of the Surface Roughness of Six Wood Species for Furniture Production on the Wettability and Bonding Quality of Coating. *Forests* **2023**, *14*, 996. [[CrossRef](#)]
43. Casilla, R.C.; Chow, S.; Steiner, P.R. An immersion technique for studying wood wettability. *Wood Sci. Technol.* **1981**, *15*, 31–43. [[CrossRef](#)]
44. Wang, X.F.; Wei, X.F.; Huang, P.Q. Study on Performance of Adherence of Water-Base UV Varnish. *Adv. Mater. Res.* **2010**, *174*, 409–413. [[CrossRef](#)]
45. Schultz, J.; Nardin, M. Theories and mechanisms of adhesion. In *Adhesion Promotion Techniques: Technological Applications*; Mittal, K.L., Pizzi, A., Eds.; Marcel Dekker: New York, NY, USA, 2002; pp. 1–26.
46. Packham, D.E. The mechanical theory of adhesion. In *Handbook of Adhesive Technology*; Pizzi, A., Mittal, K.L., Eds.; Marcel Dekker Inc.: New York, NY, USA, 2003; pp. 69–93.
47. PL234055B1. Method for Manufacturing a Cellular Plate and a Cellular Plate Manufactured by This Method. Author Maciej Tokarczyk/BORNE Furniture Comp/. Available online: <https://www.patentguru.com/PL234055B1> (accessed on 2 December 2023).

**Disclaimer/Publisher’s Note:** The statements, opinions and data contained in all publications are solely those of the individual author(s) and contributor(s) and not of MDPI and/or the editor(s). MDPI and/or the editor(s) disclaim responsibility for any injury to people or property resulting from any ideas, methods, instructions or products referred to in the content.